Nanotechnology, Science and Applications

Dovepress
Taylor & Francis Group

Open Access Full Text Article

ORIGINAL RESEARCH

Sacha Inchi Oil–Based Nanostructured Lipid Carriers for Curcumin Delivery: Development and Physicochemical Characterization

Ikra Nurohman[1,2], Anis Yohana Chaerunisaa[2], Gofarana Wilar[3], Garnadi Jafar[4], Cecep Suhandi[2], Sriwidodo Sriwidodo[2]

[1]Doctoral Program of Pharmacy, Faculty of Pharmacy, Universitas Padjadjaran, Sumedang, 45363, Indonesia; [2]Department of Pharmaceutics and Pharmaceutical Technology, Faculty of Pharmacy, Universitas Padjadjaran, Sumedang, 45363, Indonesia; [3]Department of Pharmacology and Clinical Pharmacy, Faculty of Pharmacy, Universitas Padjadjaran, Sumedang, 45363, Indonesia; [4]Department of Pharmaceutics and Pharmaceutical Technology, Faculty of Pharmacy, Universitas Bhakti Kencana, Bandung, 40614, Indonesia

Correspondence: Sriwidodo Sriwidodo, Department of Pharmaceutics and Pharmaceutical Technology, Faculty of Pharmacy, Universitas Padjadjaran, Sumedang, 45363, Indonesia, Tel +62 816-4204-079, Email sriwidodo@unpad.ac.id

Background and Objective: Curcumin exhibits potent antioxidant activity beneficial for the prevention of various degenerative diseases; however, its highly lipophilic nature and susceptibility to degradation limit its solubility and physicochemical stability. To address these limitations, curcumin was formulated into nanostructured lipid carriers (NLCs), a lipid-based colloidal delivery system composed of solid and liquid lipids stabilized by surfactants. In this study, sacha inchi oil, a natural oil rich in omega-3 and other unsaturated fatty acids, was investigated as a novel liquid lipid component to improve lipid matrix structure and drug accommodation.

Methods: Curcumin-loaded NLCs were prepared using the hot homogenization method followed by probe sonication. Curcumin served as the active compound, while solid lipids (oleum cacao, glyceryl behenate (Compritol® 888 ATO), or glyceryl palmitostearate (Precirol® ATO 5)), sacha inchi oil as the liquid lipid, and surfactants (Tween 80, Poloxamer, or a Tween 80–Span 80 combination) were used. The resulting NLCs were characterized in terms of particle size, polydispersity index (PDI), zeta potential (ZP), entrapment efficiency (EE), physicochemical properties (FTIR, DSC, XRD), morphology, and in vitro release behavior.

Results: Physicochemical analyses confirmed successful incorporation of curcumin into the lipid matrix without undesirable interactions. Among the tested formulations, CaTS2 (oleum cacao 4.5%, sacha inchi oil 1%, Tween 80 12.5%, Span 80 1%, and curcumin 0.1%) demonstrated the most favorable characteristics, with a particle size of 95.50 ± 0.87 nm, PDI of 0.119 ± 0.157, and ZP of −22.30 ± 0.98 mV. Entrapment efficiency reached 97.24% and morphological analysis showed predominantly spherical particles. In vitro release exhibited a biphasic pattern, consisting of an initial burst followed by sustained release up to 480 min. Kinetic modeling revealed that CaTS2 followed the Korsmeyer–Peppas model (R^2 = 0.793; n = 0.301), consistent with Fickian diffusion, whereas pure curcumin followed the Higuchi model (R^2 = 0.819). The similarity factor (f_2 = 29.04) indicated a distinctly different release profile between the two systems.

Conclusion: Sacha inchi oil–based nanostructured lipid carriers were successfully developed and demonstrated favorable physicochemical characteristics, supporting their potential as a stable delivery system for curcumin.

Keywords: curcumin, nanostructured lipid carriers, sacha inchi oil, drug delivery, lipid-based nanoparticle

Introduction

Curcumin is the principal bioactive constituent of *Curcuma longa* and has long been recognized for its broad spectrum of therapeutic effects.[1] Its biological activities include antioxidant, anti-inflammatory, and anticancer properties, as well as potential roles in the prevention of degenerative diseases.[2] Despite these promising pharmacological attributes, the application of curcumin in pharmaceutical and healthcare fields remains substantially limited.[3] The major challenges associated with curcumin utilization arise from its highly lipophilic nature, poor aqueous solubility, and susceptibility to degradation when exposed to light, heat, or unfavorable pH conditions.[4] These factors contribute to the physicochemical

https://doi.org/10.2147/NSA.S589429
Received: 16 December 2025
Accepted: 19 March 2026
Published: 16 April 2026

instability of curcumin and reduce its effectiveness when formulated using conventional dosage forms.[5] Consequently, curcumin exhibits low bioavailability in vivo, despite its high intrinsic biological potential.[6]

One effective strategy to overcome these limitations is the application of nanoparticle-based drug delivery systems.[7] This approach enables compounds to be formulated at the nanometer scale (1–100 nm), where physicochemical properties differ significantly from bulk materials due to increased surface area-to-volume ratio and altered interfacial behavior.[8] Furthermore, the reduced particle size facilitates interaction with lipid membranes, which can enhance solubility and bioavailability of lipophilic compounds such as curcumin.[9] Among various nanoparticle delivery systems, nanostructured lipid carriers (NLCs) have emerged as a widely investigated platform for the delivery of lipophilic compounds.[10] NLCs consist of a mixture of solid and liquid lipids stabilized by surfactants, forming a stable colloidal system.[11] Compared with solid lipid nanoparticles (SLNs), NLCs possess a more flexible internal structure with lower crystallinity, allowing improved drug incorporation and enhanced physical and chemical stability.[12] The advantages of NLCs extend beyond their stability, as they are capable of preventing lipid recrystallization and increasing drug loading efficiency.[13] This structural characteristic provides enhanced protection of lipophilic compounds such as curcumin against degradation, thereby improving formulation quality and therapeutic potential.[14] Beyond structural advantages, NLCs have been widely investigated for multiple pharmaceutical and cosmetic applications, including oral delivery to improve the bioavailability of poorly soluble drugs, topical and transdermal systems to enhance dermal penetration, ocular formulations, and controlled-release systems.[15] Their ability to protect encapsulated compounds from chemical degradation and modulate release profiles further supports their versatility as delivery platforms for lipophilic bioactives such as curcumin. Accordingly, NLCs are considered one of the most promising delivery systems for curcumin-based formulations.[16]

In the development of NLCs, the selection of liquid lipids plays a critical role in determining formulation performance.[17] In this study, sacha inchi oil, which is rich in polyunsaturated fatty acids (omega-3, omega-6, and omega-9), was selected as the liquid lipid component.[18] In addition to supporting NLC structural formation, sacha inchi oil exhibits intrinsic antioxidant activity, which may provide added functional benefits.[19] Its incorporation is therefore expected to exert synergistic effects with curcumin in enhancing overall pharmacological performance.[20] However, despite the growing interest in natural oils for lipid-based nanocarriers, studies specifically investigating sacha inchi oil as a liquid lipid in nanostructured lipid carrier systems for curcumin delivery remain limited. Beyond lipid selection, the success of NLC formulations is strongly influenced by the type of surfactant employed.[11] Surfactants play a crucial role in reducing interfacial tension between lipid and aqueous phases, thereby facilitating the formation of smaller and more stable particle dispersions.[21] In the present study, Tween 80, Poloxamer 188, and a combination of Tween 80 and Span 80 were utilized. Tween 80 is a nonionic surfactant known for its effective stabilizing properties,[22] while Poloxamer 188 contributes to improved thermodynamic stability of the system.[23] The combination of Tween 80 and Span 80 provides a synergistic effect through balanced hydrophilic–lipophilic balance (HLB) values, which support emulsion stability.[24] Accordingly, these surfactant variations are expected to produce NLCs with uniform particle size distribution, high stability, and optimal curcumin entrapment efficiency.[25]

The selection of solid lipids is another fundamental aspect in NLC formulation development.[26] Solid lipids serve as the primary matrix for encapsulating and protecting active compounds within the NLC structure.[27] In this study, oleum cacao, glyceryl behenate (Compritol® 888 ATO), and glyceryl palmitostearate (Precirol® ATO) were employed as solid lipid components. Oleum Cacao is known for its biocompatibility and widespread use in topical and oral formulations.[28] Glyceryl behenate offers high stability and an appropriate melting point for nanoparticle formation,[29] whereas glyceryl palmitostearate provides a more amorphous matrix, enhancing drug loading capacity and reducing the risk of crystallization.[30] The complementary characteristics of these solid lipids enable the development of NLC systems that are not only physically stable but also capable of improving curcumin bioavailability.[31]

Therefore, the present study aimed to develop and systematically characterize curcumin-loaded nanostructured lipid carriers incorporating sacha inchi oil as a natural liquid lipid component. The specific objectives were to (i) evaluate the compatibility and solid-state characteristics of curcumin within different lipid matrices, (ii) determine the most suitable formulation based on physicochemical characteristics, and (iii) assess particle size distribution, zeta potential (ZP), entrapment efficiency (EE), morphology, and in vitro release behavior. It is anticipated that the findings of this study will contribute to the advancement of lipid-based drug delivery systems utilizing natural lipids and support their potential application in stable and effective pharmaceutical and cosmetic products.

Materials and Methods

Materials

The primary material used in this study was curcumin as the active compound. Curcumin was obtained from a chemical industry supplier with pharmaceutical-grade quality. Preliminary evaluation of the active compound was conducted by verifying the completeness and validity of the Certificate of Analysis (CoA) provided by the supplier to ensure quality and purity. Glyceryl behenate and glyceryl palmitostearate were kindly supplied by Gattefossé (Saint-Priest, France). Oleum cacao (pharmaceutical grade) was obtained from a certified local pharmaceutical raw material distributor. Sacha inchi oil (cold-pressed, pharmaceutical/cosmetic grade) was procured from a certified supplier and stored under light-protected conditions at 4°C prior to use to prevent oxidative degradation. Tween 80 (polysorbate 80) and Span 80 (sorbitan monooleate) were purchased from Merck (Darmstadt, Germany). Poloxamer 188 was obtained from BASF (Ludwigshafen, Germany). Methanol (HPLC grade) was purchased from Merck (Darmstadt, Germany) and used for analytical purposes. Distilled water was prepared in-house and used as the aqueous phase throughout the study. All materials were used as received without further purification.

Methods

Fourier Transform Infrared (FTIR) Analysis

FTIR analysis was performed to evaluate compatibility and potential interactions among formulation components.[32] The samples analyzed included solid lipids, mixtures of solid and liquid lipids, and mixtures of the active compound with solid lipids. The samples were finely ground prior to analysis and examined using an Agilent Cary 630 FTIR spectrometer. Absorption spectra were recorded to identify any peak shifts or changes indicative of physicochemical interactions.[8]

X-Ray Diffraction (XRD) Analysis

Samples subjected to XRD analysis included: (1) pure curcumin; (2) individual solid lipids (glyceryl behenate, glyceryl palmitostearate, or oleum cacao); and (3) mixtures of solid lipids with curcumin, as well as ternary mixtures consisting of solid lipid, sacha inchi oil, and curcumin. Each sample was heated until melted to obtain a homogeneous phase and subsequently allowed to solidify at room temperature. The solidified samples were then finely ground prior to analysis.[10]

XRD patterns were recorded using an X-ray diffractometer (PANalytical X'Pert PRO, Malvern Panalytical, The Netherlands) equipped with Cu Kα radiation (λ = 1.5406 Å), operated at 40 kV and 30 mA. Diffraction data were collected over a 2θ range of 5–70° at a scanning rate of 2°/min. The obtained diffractograms were analyzed to evaluate crystallinity and possible structural changes in the lipid matrix after curcumin incorporation. It should be noted that the analyzed samples represent bulk lipid mixtures rather than dispersed nanoparticles. This approach was intended to evaluate intrinsic crystallinity behavior and lipid–drug interactions at the matrix level, rather than structural transitions occurring in the colloidal state.

Differential Scanning Calorimetry (DSC)

DSC analysis was conducted to investigate the thermal properties of individual components and their mixtures within the formulation. Approximately 5–10 mg of each sample, including solid lipids and their mixtures with curcumin, were accurately weighed and sealed in aluminum pans. Thermal analysis was performed using a DSC instrument (DSC 60 Plus, Shimadzu Corporation, Kyoto, Japan) under a nitrogen purge (50 mL/min).

The temperature was increased from 30 to 300 °C at a heating rate of 10 °C/min. An empty sealed aluminum pan was used as a reference. The resulting thermograms provided thermal parameters, including onset temperature, melting peak temperature, and enthalpy change (ΔH), which were used to assess potential interactions and crystallinity changes in the lipid matrix.[8] The thermal analysis focused on bulk systems to investigate matrix-level interactions. Future studies may consider freeze-dried nanoparticle analysis to more closely reflect the dispersed nanostructured state.

Preparation of Curcumin-Loaded Nanostructured Lipid Carriers

Curcumin-loaded NLCs were prepared using the hot homogenization method followed by probe sonication. The selection of lipid components and surfactant systems was based on previously reported curcumin-loaded NLC formulations and

preliminary compatibility studies.[33–35] The solid lipids (oleum cacao, glyceryl behenate, and glyceryl palmitostearate) were selected to represent matrices with different crystallinity profiles, while sacha inchi oil was incorporated as a liquid lipid due to its high unsaturation degree, which is expected to modulate lipid matrix packing and enhance drug accommodation. Surfactant types (Tween 80, Poloxamer 188, and Tween 80–Span 80 combination) and their concentration ranges were chosen based on literature reports demonstrating effective interfacial stabilization of lipid nanoparticles within similar composition windows. The qualitative and quantitative composition of each formulation is summarized in Table 1.

Solid lipids (oleum cacao, glyceryl behenate, or glyceryl palmitostearate) were mixed with curcumin and melted, followed by magnetic stirring for 15 min until a homogeneous lipid phase was obtained.[10] The lipid phase containing sacha inchi oil as the liquid lipid was heated concurrently with the aqueous phase containing the surfactant (Tween 80, Poloxamer 188, or a Tween 80–Span 80 combination). The two phases were then combined and subjected to particle size reduction using a probe ultrasonicator at 60% amplitude for 15 min under temperature-controlled conditions at 70°C.[36] The resulting NLC dispersion appeared turbid to milky white without visible phase separation and was subsequently used for characterization studies.

Characterization of Curcumin-Loaded NLCs

The physicochemical stability of curcumin-loaded NLCs during storage was evaluated using a Malvern Zetasizer ZSP (UK). Characterization parameters included particle size, polydispersity index (PDI), and ZP. EE was determined using ultracentrifugation and centrifugal ultrafiltration device (Vivaspin®).[37] The physicochemical stability was monitored for 30 days under controlled room temperature conditions (25°C). The stability evaluation was intended as a preliminary short-term assessment to observe physical integrity over one month, rather than to establish definitive long-term shelf-life or mechanistic stability predictions. All experiments were performed in triplicate (n = 3), and results are expressed as mean ± standard deviation (SD). Statistical analysis was conducted using one-way analysis of variance (ANOVA) followed by Tukey's post hoc test for normally distributed data. For non-normally distributed data, the Kruskal–Wallis test followed by Dunn's post hoc test with Bonferroni correction was applied. A p-value < 0.05 was considered statistically significant.

Particle Size and Polydispersity Index

Particle size and PDI measurements were performed by diluting the NLC dispersion at a fixed ratio of 1:100 (v/v) with distilled water prior to analysis. The diluted sample was transferred into a disposable cuvette for analysis. This standardized dilution ratio was selected to minimize multiple scattering effects and ensure reproducible measurements. Measurements were conducted using the Malvern Zetasizer ZSP.[8,10]

Zeta Potential Measurement

ZP was measured using a Malvern Zetasizer ZSP (UK) at room temperature (±25 °C). The NLC dispersion was diluted at a fixed ratio of 1:100 (v/v) with distilled water prior to ZP measurement to ensure reproducibility and adequate signal detection. The diluted sample was then transferred into a disposable cuvette for analysis.[8,10]

Entrapment Efficiency (EE)

EE was determined by loading 1 mL of curcumin-loaded NLC dispersion into a centrifugal filter unit (Goettingen, Germany) equipped with a 5 kDa molecular weight cut-off membrane.[37] The samples were centrifuged at 14,500 rpm for 3 h. Prior to ultrafiltration, the dispersion was visually inspected to ensure absence of visible drug crystals. The 5 kDa molecular weight cut-off membrane was selected to allow passage of dissolved free curcumin while retaining nanoparticle-associated drug. The method was performed under high centrifugal force and extended duration to minimize retention of unencapsulated drug aggregates. The collected filtrate (supernatant) was appropriately diluted and analyzed using a UV–Vis spectrophotometer (Shimadzu UV-1800) at the maximum absorption wavelength of curcumin.[38] The concentration of free (non-encapsulated) curcumin was calculated, and EE was determined using the following equation:

$$\%EE = \frac{\text{Total amount of curcumin} - \text{Free curcumin}}{\text{Total amount of curcumin}} \times 100\%$$

Table 1 Formulation Composition and Physicochemical Characterization of Curcumin-Loaded Nanostructured Lipid Carriers (NLCs) on Day 1, Including Particle Size, PDI, ZP, and EE

Formulation									Particle Size (nm)	ZP (mV)	PDI	EE (%)
Code	Cur (%)	MSI (%)	CMP (%)	PRE (%)	OLC (%)	Tween (%)	Span (%)	PLX (%)				
CT2	0,1	1	–	–	4,5	12,5	–	–	64.54 ± 1.83	−30.07 ± 1.01	0.345 ± 0.337	94.604 ± 1.108
CoT2	0,1	1	4,5	–	–	12,5	–	–	551.73 ± 147.83	−48.87 ± 0.70	1.000 ± 0.000	81.405 ± 0.250
PrT2	0,1	1	–	4,5	–	12,5	–	–	75.78 ± 3.69	−26.87 ± 1.99	0.355 ± 0.363	80.286 ± 0.623
PrP2	0,1	1	–	4,5	–	–	–	2,5	434.23 ± 207.86	−14.83 ± 0.50	0.680 ± 0.563	96.124 ± 1.455
CaTS2	0,1	1	–	–	4,5	12,5	1	–	95.50 ± 0.87	−22.30 ± 0.98	0.119 ± 0.157	97.244 ± 0.069
PreTS2	0,1	1	–	4,5	–	12,5	1	–	131.60 ± 55.46	−31.63 ± 1.46	0.360 ± 0.404	96.644 ± 0.069

Note: Data are presented as mean ± SD (n = 3) for particle size, PDI, ZP, and EE.

Abbreviations: Cur, Curcumin; MSI, Minyak Sacha Inchi; CMP, glyceryl behenate; Pre, glyceryl palmitostearate; OLC, oleum cacao; PLX, Poloxamer; PDI, Polydispersity Index; ZP, Zeta Potential; EE, Entrapment Efficiency.

https://doi.org/10.2147/NSA.S589429

Transmission Electron Microscopy (TEM)

The morphology of the curcumin-loaded nanostructured lipid carriers was examined using low-resolution transmission electron microscopy (LRTEM; JEM-1400, JEOL Ltd., Tokyo, Japan) operated at an accelerating voltage of 80 kV.[39] A representative NLC formulation showing the most favorable physicochemical characteristics (based on particle size, PDI, ZP, and EE) was selected for TEM analysis. A drop of the selected NLC dispersion was diluted with distilled water and placed onto a carbon-coated copper grid. Excess liquid was carefully removed using filter paper, and the sample was allowed to air-dry at room temperature. For contrast enhancement, the sample was negatively stained with 2% (w/v) phosphotungstic acid prior to imaging. Micrographs were captured to observe particle morphology, surface characteristics, and approximate size distribution.

In vitro Release Study

The in vitro release of curcumin from the NLC formulations was evaluated using a dialysis bag diffusion method with minor modifications.[40,41] Release experiments were conducted in triplicate (n = 3), and cumulative release values are presented as mean ± SD. The dialysis membrane (molecular weight cut-off [MWCO] 12,000–14,000 Da) was pre-soaked in phosphate buffer (pH 7.4) for 24 h prior to the experiment to ensure proper membrane hydration. An aliquot of curcumin-loaded NLC dispersion, equivalent to a predetermined amount of curcumin (1.25 mg), was placed into the dialysis bag, which was securely sealed at both ends. The dialysis bag was then immersed in 40 mL of phosphate buffer (pH 7.4) as the release medium in a beaker and maintained at 37 ± 0.5 °C under continuous magnetic stirring at 50 rpm to simulate physiological conditions. The release medium volume (40 mL) was selected to maintain sink conditions, defined as a volume at least three times higher than that required to dissolve the total amount of curcumin loaded (1.25 mg), considering the limited aqueous solubility of curcumin.

At predetermined time intervals (15, 30, 45, 60, 90, 120, 240, 360, and up to 480 min), 1 mL aliquots of the release medium were withdrawn and immediately replaced with an equal volume of fresh phosphate buffer maintained at the same temperature. The collected samples were filtered or centrifuged, when necessary, to remove any residual lipid nanoparticles.

The concentration of released curcumin was determined using UV–Vis spectrophotometry at its maximum absorption wavelength ($\lambda\_max \approx 425$ nm). The cumulative percentage of curcumin released was calculated based on the total amount of curcumin initially loaded in the NLC formulation and plotted as a function of time to obtain the in vitro release profile.

To elucidate the release mechanism, the dissolution data were further fitted to various kinetic models, including Zero-order, First-order, Higuchi, and Korsmeyer–Peppas models. The coefficient of determination (R^2) was used to evaluate the goodness of fit, and the diffusional exponent (n) derived from the Korsmeyer–Peppas model was employed to characterize the release mechanism (Fickian or non-Fickian transport). Model fitting was performed using linear regression analysis of the appropriately transformed dissolution data.[42]

Additionally, the similarity factor (f_2) was calculated to quantitatively compare the dissolution profiles between pure curcumin and the selected formulation. The f_2 value was determined using the standard logarithmic equation recommended by regulatory guidelines, based on the mean cumulative percentage release at each sampling time point. An f_2 value between 50 and 100 was considered indicative of similar release profiles.[43]

Results and Discussion

FT-IR Analysis

FT-IR spectroscopy was performed to evaluate potential chemical interactions between curcumin and the lipid components (oleum cacao, glyceryl behenate, glyceryl palmitostearate, and sacha inchi oil). The spectra are presented in Figure 1A–C. Pure curcumin (Figure 1A(i)–C(i)) displayed characteristic bands at ~1624–1626 cm^{-1} (aromatic C=C and conjugated C=O stretching), ~1508–1510 cm^{-1} (benzene ring vibration), and ~1270–1280 cm^{-1} (phenolic C–O stretching), with additional C–O–C absorptions at ~1110–1150 cm^{-1}. A broad band at ~3400–3500 cm^{-1} corresponded to O–H stretching.[10]

The pure solid lipids (Figure 1A(ii)–C(ii)) exhibited typical ester functional group absorptions, including a strong carbonyl (C=O) band at ~1728–1732 cm^{-1}, CH_2 bending at ~1465–1470 cm^{-1}, and C–O stretching at ~1100–1180 cm^{-1}. In the physical mixtures (Figure 1A(iii)–C(iii)), the spectra showed superimposed peaks of curcumin and the respective lipids. The

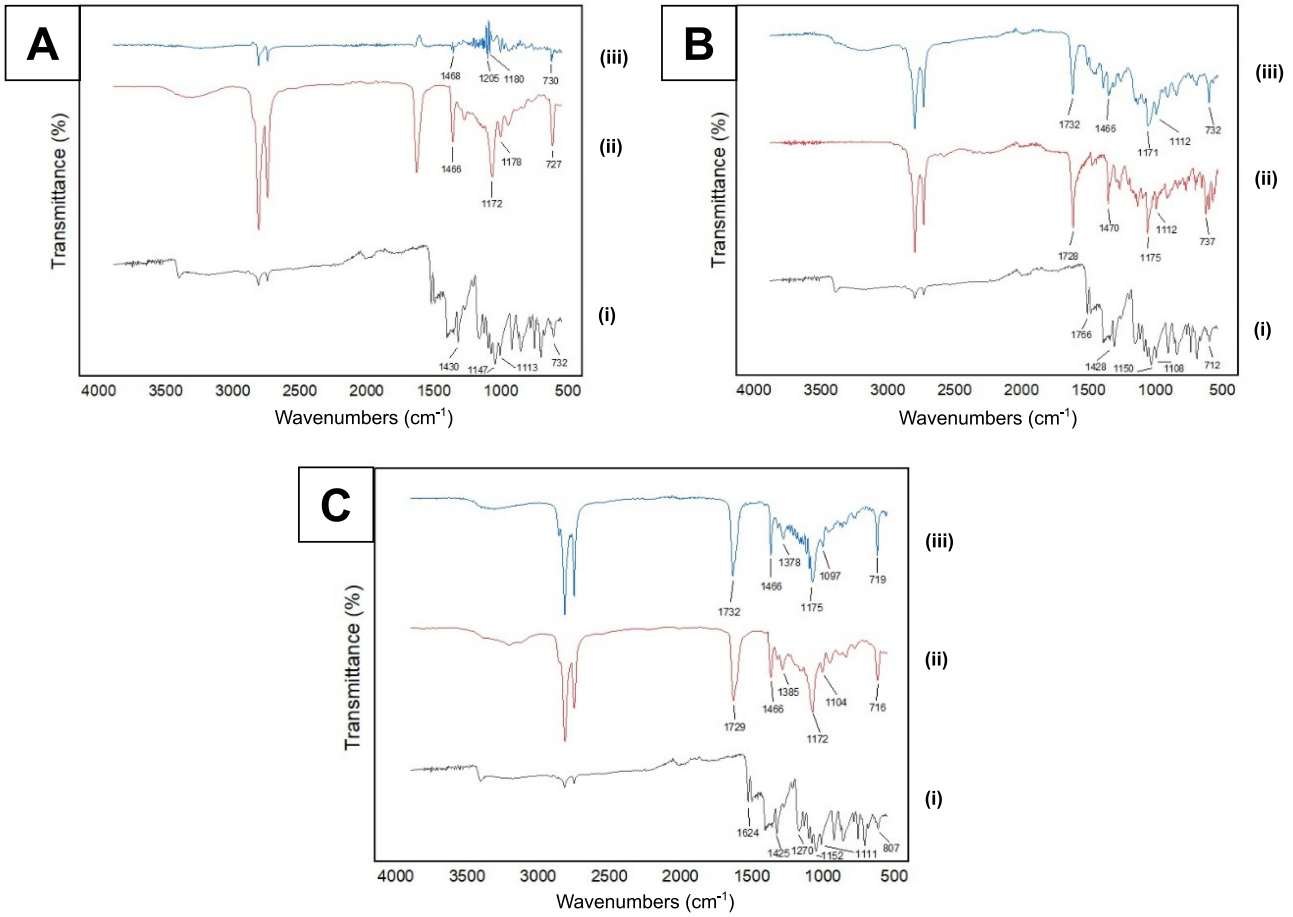

Figure 1 FT-IR absorption spectra of curcumin, solid lipids, and their lipid mixtures. (**A**) Glyceryl behenate–based system: (i) pure curcumin, (ii) glyceryl behenate, and (iii) physical mixture of glyceryl behenate, sacha inchi oil, and curcumin. (**B**) Oleum cacao–based system: (i) pure curcumin, (ii) oleum cacao, and (iii) physical mixture of oleum cacao, sacha inchi oil, and curcumin. (**C**) Glyceryl palmitostearate–based system: (i) pure curcumin, (ii) glyceryl palmitostearate, and (iii) physical mixture of glyceryl palmitostearate, sacha inchi oil, and curcumin.

characteristic curcumin band at ~1625 cm^{-1} remained detectable alongside the lipid carbonyl peak at ~1730 cm^{-1}, without new bands or significant shifts ($\Delta < 5–10\ cm^{-1}$). These findings indicate the absence of covalent interactions, suggesting good physicochemical compatibility and preservation of curcumin integrity within the lipid matrices.

X-Ray Diffraction (XRD) Analysis

The crystalline characteristics of curcumin upon incorporation into the lipid matrix were evaluated by XRD (Figure 2A–C). Pure curcumin (Figure 2A(i)–C(i)) exhibited multiple sharp diffraction peaks, confirming its crystalline nature. A prominent reflection was observed at approximately $2\theta \approx 17.4°$, together with additional peaks, indicating a well-ordered crystal lattice.[8]

The pure solid lipids (Figure 2A(ii)–C(ii)) displayed characteristic diffraction peaks within the range of approximately 19–26°, consistent with their crystalline lipid structures. Compared with pure curcumin, the solidified lipid mixtures (Figure 2A(iii)–C(iii)) showed attenuation or disappearance of the distinctive curcumin peak at ~17.4°. The diffraction patterns of the mixtures were primarily dominated by lipid-associated reflections, with reduced intensity of curcumin-specific peaks. The diminished intensity and partial loss of curcumin reflections indicate a reduction in crystallinity following incorporation into the lipid matrices. This suggests partial amorphization and molecular dispersion of curcumin within the lipid lattice rather than the presence of intact crystalline drug domains.[10]

https://doi.org/10.2147/NSA.S589429

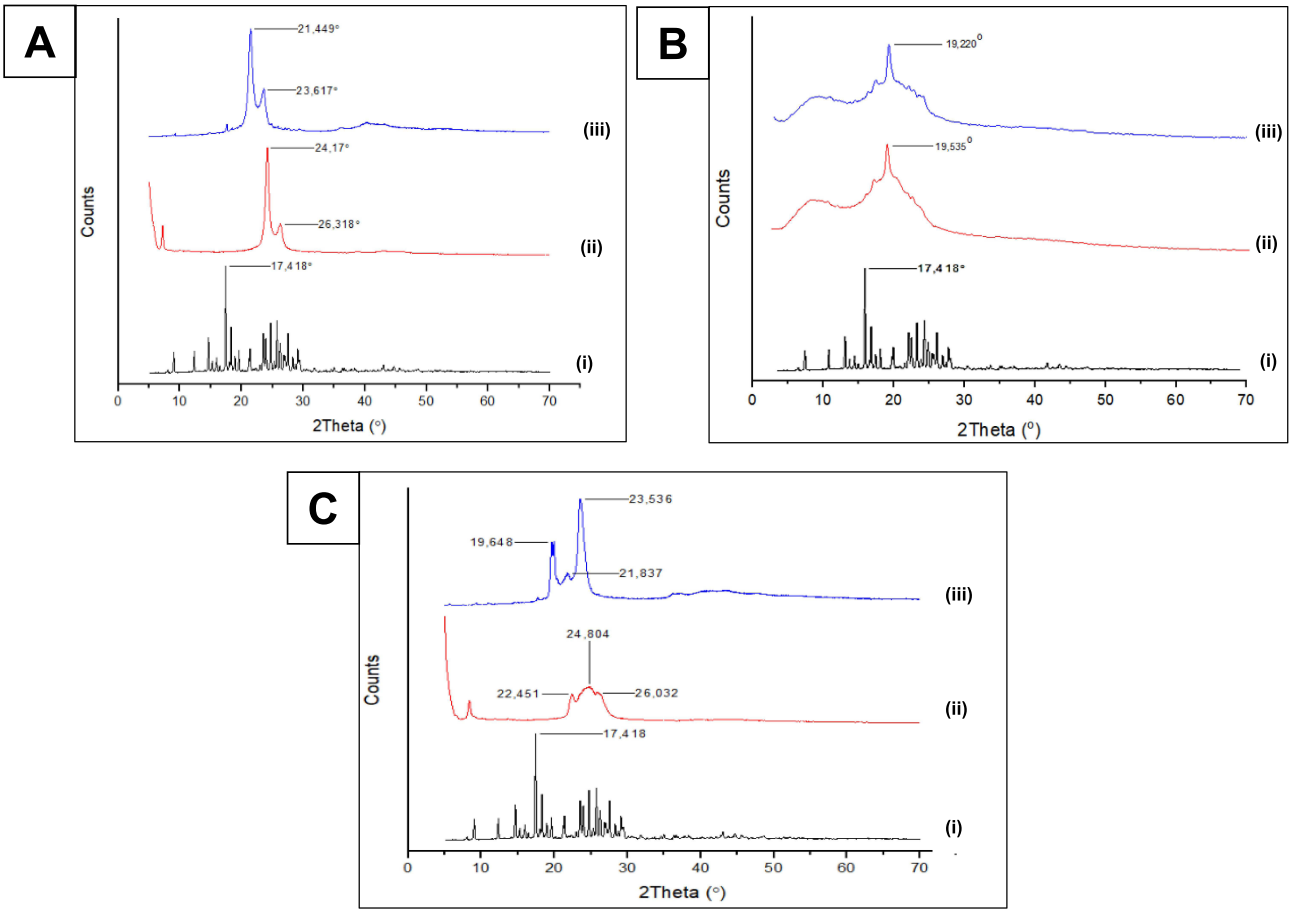

Figure 2 X-ray diffraction (XRD) patterns of curcumin, solid lipids, and their lipid mixtures. (**A**) Glyceryl behenate–based system: (i) pure curcumin, (ii) glyceryl behenate, and (iii) solidified mixture of glyceryl behenate, sacha inchi oil, and curcumin. (**B**) Oleum cacao–based system: (i) pure curcumin, (ii) oleum cacao, and (iii) solidified mixture of oleum cacao, sacha inchi oil, and curcumin. (**C**) Glyceryl palmitostearate–based system: (i) pure curcumin, (ii) glyceryl palmitostearate, and (iii) solidified mixture of glyceryl palmitostearate, sacha inchi oil, and curcumin.

Additionally, the presence of sacha inchi oil, rich in polyunsaturated fatty acids, may contribute to lattice imperfections within the solid lipid matrix, thereby facilitating drug dispersion and supporting the reduced crystallinity observed in the solidified mixtures.[44] Moreover, the absence of distinct crystalline drug peaks suggests effective incorporation of curcumin within the lipid framework. Collectively, these structural changes support the successful integration of curcumin into the solidified lipid matrices, enhancing formulation homogeneity and overall functional performance.

Differential Scanning Calorimetry (DSC) Analysis

DSC thermograms (Figure 3A–C) were used to evaluate solid-state changes of curcumin after incorporation into the lipid matrices. Pure curcumin (Figure 3A(i)–C(i)) exhibited a sharp endothermic melting peak at approximately 158.2 °C, confirming its crystalline nature. Each solid lipid showed its characteristic melting transition: glyceryl behenate at ~71.9 °C (Figure 3A(ii)), oleum cacao at ~26.9 °C (Figure 3B(ii)), and glyceryl palmitostearate at ~64.2 °C (Figure 3C(ii)).

In the lipid–curcumin mixtures (Figure 3A(iii)–C(iii)), the melting endotherm of curcumin at ~158 °C was absent. Instead, the thermograms were dominated by lipid melting transitions, with slight temperature shifts compared to the respective pure lipids (eg, ~80.0 °C for glyceryl behenate mixture and ~70.3 °C for glyceryl palmitostearate mixture). The disappearance of the curcumin melting peak indicates it is no longer present as a separate crystalline phase but dispersed within the lipid matrix. These findings are consistent with the XRD data showing attenuation of curcumin diffraction peaks, collectively suggesting reduced crystallinity and partial amorphization after incorporation into the lipid systems. Such modification may enhance drug dispersion and physicochemical stability in lipid-based formulations.[44]

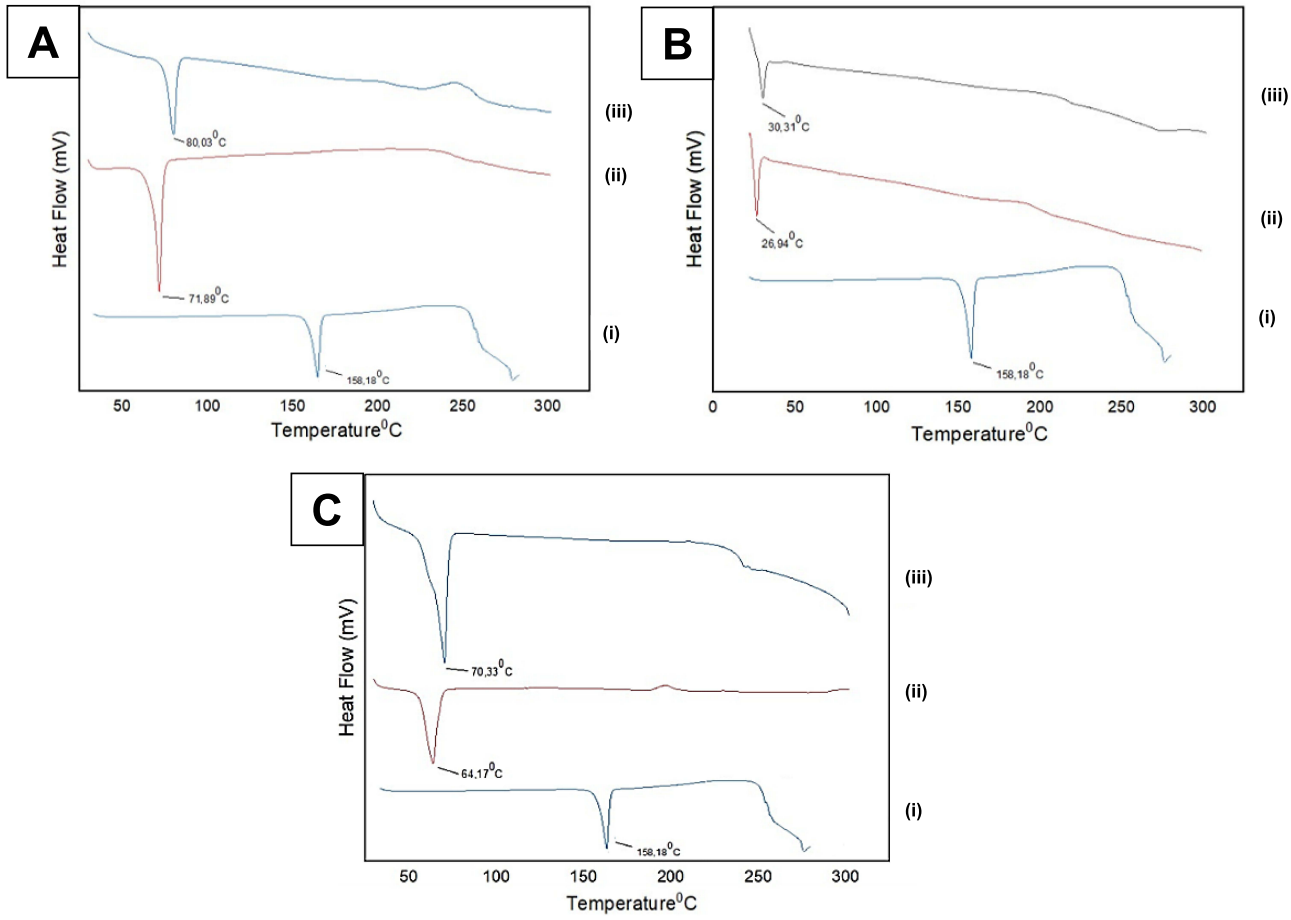

Figure 3 Differential scanning calorimetry (DSC) thermograms of curcumin, solid lipids, and lipid–curcumin mixtures. (**A**) Glyceryl behenate–based system: (i) pure curcumin, (ii) glyceryl behenate, and (iii) lipid–curcumin mixture. (**B**) Oleum cacao–based system: (i) pure curcumin, (ii) oleum cacao, and (iii) lipid–curcumin mixture. (**C**) Glyceryl palmitostearate–based system: (i) pure curcumin, (ii) glyceryl palmitostearate, and (iii) lipid–curcumin mixture.

Physicochemical Characterization of Curcumin NLC

The physicochemical properties of curcumin-loaded NLC formulations were evaluated in terms of particle size, PDI, ZP, and EE,[45] as summarized in Table 1 and Table 2.

Particle Size and Polydispersity Index

The majority of formulations exhibited particle sizes below 500 nm on day 1, indicating successful formation of nanoscale lipid carriers through the hot homogenization–ultrasonication method.[8] The notably smaller particle sizes observed in CT2, PrT2, CaTS2, and PreTS2 (<150 nm) can be attributed to the synergistic effect between the solid lipid matrix and the selected surfactant systems, which effectively reduced interfacial tension and stabilized newly formed nanoparticles during high-energy processing.[46] In particular, the combination of Tween 80 and Span 80 likely contributed to improved interfacial packing due to their complementary hydrophilic–lipophilic balance (HLB) values, resulting in more compact and uniform particles.[47]

During the preliminary screening phase, the glyceryl behenate-based formulation (CoT2) exhibited particle size values comparable to the other formulations at day 0; however, it presented an extremely high PDI (≈1), indicating a highly polydisperse and heterogeneous system. Despite the acceptable mean particle size, such a broad distribution profile reflects poor colloidal uniformity and instability. Therefore, CoT2 was excluded from subsequent investigation and long-term evaluation.

In contrast, PrP2 exhibited a substantially larger particle size, suggesting inadequate interfacial stabilization. This behavior may be related to the higher crystallinity of glyceryl palmitostearate combined with Poloxamer, which could

Table 2 Formulation Composition and Physicochemical Characterization of Curcumin-Loaded Nanostructured Lipid Carriers (NLCs) After 30 days of Storage at Room Temperature, Including Particle Size, PDI, ZP, and EE

Formulation									Particle Size (nm)	ZP (mV)	PDI	EE (%)
Code	Cur (%)	MSI (%)	CMP (%)	PRE (%)	OLC (%)	Tween (%)	Span (%)	PLX (%)				
CT2	0,1	1	–	–	4,5	12,5	–	–	56.37 ± 0.52	−19.57 ± 3.00	0.237 ± 0.014	93.485 ± 0.416
CoT2	0,1	1	4,5	–	–	12,5	–	–	–	–	–	–
PrT2	0,1	1	–	4,5	–	12,5	–	–	88.93 ± 3.43	−25.43 ± 1.25	0.515 ± 0.050	74.006 ± 1.316
PrP2	0,1	1	–	4,5	–	–	–	2,5	3110.67 ± 728.6	−5.02 ± 0.22	0.053 ± 577.3	96.804 ± 0.069
CaTS2	0,1	1	–	–	4,5	12,5	1	–	89.37 ± 1.83	−20.23 ± 0.61	0.079 ± 0.038	97.164 ± 0.069
PreTS2	0,1	1	–	4,5	–	12,5	1	–	84.90 ± 40.28	−27.97 ± 0.83	0.177 ± 0.024	97.084 ± 0.000

Note: Data are presented as mean ± SD (n = 3) for particle size, PDI, ZP, and EE.

Abbreviations: Cur, Curcumin; MSI, Minyak Sacha Inchi; CMP, glyceryl behenate; Pre, glyceryl palmitostearate; OLC, oleum cacao; PLX, Poloxamer; PDI, Polydispersity Index; ZP, Zeta Potential; EE, Entrapment Efficiency.

https://doi.org/10.2147/NSA.S589429

limit lipid matrix flexibility and hinder efficient surfactant adsorption at the particle surface.[12] A rigid lipid core may also promote partial coalescence during cooling, leading to particle growth.[48]

Statistical analysis using one-way ANOVA demonstrated significant differences in particle size among formulations on day 1 ($p < 0.01$) and day 30 ($p < 0.001$). Post hoc Tukey analysis revealed that PrP2 exhibited significantly larger particle size compared to the other formulations ($p < 0.05$), whereas no significant differences were observed among CT2, PrT2, CaTS2, and PreTS2. These results statistically support the exclusion of PrP2 due to its markedly larger particle size.

When compared with previously reported curcumin-loaded NLCs formulated using commonly employed liquid lipids such as medium-chain triglycerides, oleic acid, or isopropyl myristate, which typically exhibit particle sizes in the range of 150–300 nm,[49–51] the smaller particle sizes (<150 nm) achieved in several sacha inchi oil–based formulations suggest that the high degree of unsaturation may facilitate more efficient lipid matrix dispersion during high-energy homogenization.[52] This indicates that sacha inchi oil performs comparably, and in certain formulations favorably, relative to conventional liquid lipids.

Changes in particle size after 30 days further reflect differences in long-term stability. The reduction in particle size observed in CT2 and PreTS2 may be explained by gradual drug diffusion from the lipid core and subsequent matrix rearrangement, leading to slight particle shrinkage.[53] Conversely, the marked particle growth in PrP2 strongly indicates aggregation or coalescence, consistent with its suboptimal surfactant coverage and unfavorable solid–liquid lipid ratio.[54] These findings highlight the importance of balancing lipid crystallinity and surfactant efficiency in influencing short-term colloidal behavior under the tested storage conditions.

PDI values supported these observations, with most formulations showing homogeneous size distribution (PDI < 0.5) on day 1.[10] Kruskal–Wallis analysis indicated a significant overall difference in PDI among formulations on day 1 ($p < 0.05$); however, no significant pairwise differences were observed after Bonferroni correction. On day 30, no statistically significant differences in PDI were detected ($p > 0.05$).

The improved PDI of CaTS2 and PreTS2 after storage may reflect internal matrix rearrangement toward a more uniform dispersion state. In contrast, the increased PDI of PrT2 may indicate partial destabilization, possibly caused by drug expulsion during lipid recrystallization.[11] Although PrP2 exhibited a lower PDI after 30 days, this likely reflects uniform aggregation of larger particles rather than genuine nanoscale stability, emphasizing that low PDI alone should not be interpreted as an indicator of formulation robustness.[55]

Zeta Potential

ZP measurements revealed that most formulations possessed surface charges exceeding −20 mV on day 1, which is generally considered sufficient to provide electrostatic repulsion and prevent particle aggregation.[8,10] The favorable ZP values observed in CT2, PrT2, CaTS2, and PreTS2 can be attributed to effective surfactant adsorption at the particle surface, creating a charged interfacial layer.[56] Although CoT2 exhibited measurable ZP at day 0, its highly polydisperse nature (PDI ≈ 1) rendered the system unsuitable for reliable long-term stability assessment; therefore, it was not further monitored at day 30.

One-way ANOVA demonstrated significant differences in ZP among formulations on both day 1 and day 30 ($p < 0.001$). Tukey's post hoc analysis indicated that PrP2 exhibited significantly lower absolute ZP values compared to the other formulations ($p < 0.05$), consistent with its greater tendency toward particle aggregation. On day 30, CaTS2 maintained significantly higher absolute ZP values compared to PrP2 and PreTS2 ($p < 0.05$), while no significant difference was observed between CaTS2 and CT2.

The gradual decrease in ZP observed during storage, particularly in CT2 and PrP2, suggests partial desorption or rearrangement of surfactant molecules over time.[57] PrP2 consistently showed the lowest absolute ZP, which explains its pronounced aggregation tendency and increased particle size. Interestingly, some formulations maintained acceptable ZP values after 30 days, indicating that steric stabilization provided by non-ionic surfactants such as Poloxamer and Tween 80 may play a complementary role alongside electrostatic effects in preserving dispersion stability.[10,29]

Overall, the stability data indicate that selected formulations, particularly CaTS2 and PreTS2, maintained nanoscale particle size, PDI values below 0.5, and acceptable ZP over the 30-day observation period, suggesting satisfactory short-term physical storage stability under the tested conditions. The absence of pronounced aggregation or phase separation

implies that the lipid–surfactant system was able to preserve colloidal integrity during storage. Nevertheless, it should be noted that the present evaluation represents short-term stability assessment, and extended long-term or accelerated stability studies would be necessary to establish definitive shelf-life projections for pharmaceutical application.

Entrapment Efficiency

The present study demonstrated consistently high EE values (>80%, reaching up to ~90%) across all curcumin-loaded NLC formulations, indicating strong affinity of curcumin toward the lipid matrices employed.[58] This behavior is expected given the highly lipophilic nature of curcumin and its preferential partitioning into lipid-based nanocarriers. The inclusion of sacha inchi oil as the liquid lipid component may contribute to improved drug accommodation within the lipid core.[44] EE of CoT2 was determined at day 0; however, further stability evaluation was not conducted due to its highly heterogeneous dispersion profile (PDI ≈ 1), which limited its suitability for advanced characterization.

Kruskal–Wallis analysis revealed significant overall differences in EE among formulations on both day 1 ($p < 0.05$) and day 30 ($p < 0.01$). Dunn's post hoc test with Bonferroni correction indicated that CaTS2 exhibited significantly higher EE compared to PrT2 ($p < 0.05$), whereas no other pairwise comparisons showed statistically significant differences. These findings suggest that, although EE values were generally high across formulations, PrT2 demonstrated comparatively lower encapsulation performance.

Comparable findings were reported by Araujo et al, who observed EE values of 88–94% for curcumin-loaded NLCs formulated with glyceryl behenate and different liquid lipids.[49] In their study, higher EE and drug loading were attributed to a less-ordered lipid matrix, which provided greater spatial availability for curcumin incorporation. A similar mechanism is likely operative in the current formulations, where the inclusion of sacha inchi oil—rich in polyunsaturated fatty acids—may disrupt the crystalline packing of solid lipids, thereby generating lattice imperfections that favor drug entrapment.[59]

Mechanistically, the high degree of unsaturation in sacha inchi oil reduces van der Waals interactions between lipid chains, leading to increased matrix fluidity and free volume within the lipid core.[60] This structural flexibility enhances the accommodation of lipophilic molecules such as curcumin and minimizes drug expulsion during cooling and recrystallization processes. Such behavior supports the role of sacha inchi oil as a functional lattice modifier rather than merely a passive liquid lipid component.

Notably, in the present study, formulations based on glyceryl palmitostearate maintained high EE even when colloidal stability parameters (particle size and ZP) were less favorable. This observation supports previous reports suggesting that EE is not solely governed by dispersion stability, but also by the intrinsic crystallinity and polymorphic behavior of the solid lipid.[46] Glyceryl palmitostearate is known to form a relatively rigid lipid matrix, which can effectively retain lipophilic drugs within the core despite surface instability.[46] This finding is in line with Araujo et al, who emphasized that the crystalline state of the lipid matrix is a decisive factor controlling drug loading and retention.

Furthermore, the sustained EE observed in formulations containing mixed surfactant systems (Tween 80–Span 80) suggests that optimal interfacial stabilization reduces premature drug expulsion during storage.[47] Collectively, these results suggest that the interaction between solid lipid type, liquid lipid composition, and surfactant selection plays an important role in determining encapsulation performance of curcumin-loaded NLCs. From a formulation perspective, this finding highlights the potential of incorporating highly unsaturated natural oils to tailor internal lipid architecture and optimize drug loading capacity in NLC-based delivery systems. It should be noted that the present stability evaluation was limited to particle size, PDI, and ZP over 30 days; therefore, further studies incorporating additional stability metrics would provide deeper mechanistic insight.

Morphological Evaluation

TEM analysis of the selected formulation exhibiting the most favorable physicochemical characteristics (CaTS2) revealed spherical nanoparticles with smooth surfaces and relatively uniform size distribution (Figure 4). This morphology is characteristic of well-formed NLC systems and corroborates the particle size and PDI data obtained by dynamic light scattering.[61] The absence of irregular shapes or collapsed structures suggests that the lipid matrix remained intact during formulation and storage. The spherical morphology also supports the high EE and controlled release behavior observed, as uniform particles are known to promote predictable diffusion pathways for encapsulated drugs. The uniform

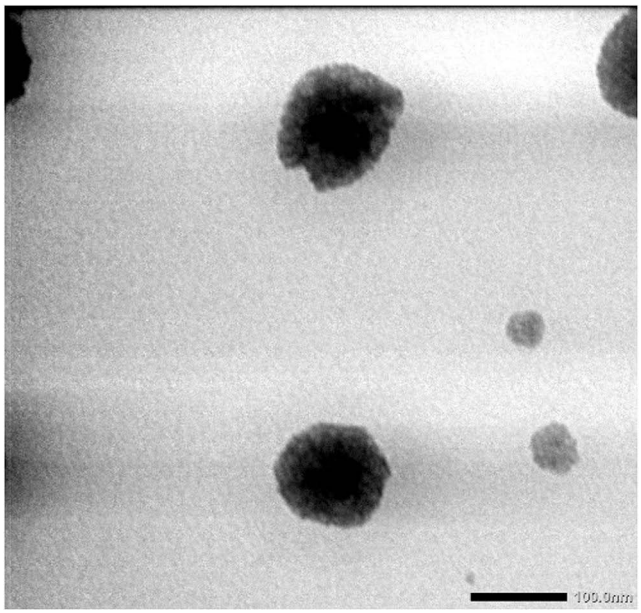

Figure 4 Transmission electron microscopy (TEM) micrograph of the selected curcumin-loaded nanostructured lipid carrier formulation (CaTS2), showing predominantly spherical nanoparticles with smooth surfaces. Scale bar: 100 nm.

spherical morphology and smooth surface further suggest that the inclusion of sacha inchi oil did not compromise structural integrity, but instead contributed to a balanced lipid organization capable of maintaining nanoscale stability.

In vitro Release Study

The in vitro release profiles revealed distinct release behaviors between the selected formulation and the unloaded curcumin, underscoring the influence of lipid composition on curcumin diffusion kinetics (Figure 5). CaTS2, the selected formulation, exhibited a biphasic release pattern, characterized by an initial burst release (~40% within the first 60–90 minutes),[62] followed by a slower and sustained release phase up to 480 minutes. This release profile is typical of NLC systems and can be attributed to the presence of curcumin molecules weakly associated with or adsorbed onto the particle surface, which are rapidly released upon contact with the dissolution medium. In contrast, pure curcumin displayed markedly slower release behavior, with cumulative release limited to approximately 15–20% over the same period.

To further elucidate the underlying release mechanisms, the dissolution data were fitted to Zero-order, First-order, Higuchi, and Korsmeyer–Peppas kinetic models (Table 3). For pure curcumin, the Higuchi model provided the best fit ($R^2 = 0.819 \pm 0.060$), indicating diffusion-controlled release from a poorly soluble matrix. In contrast, CaTS2 showed the highest correlation with the Korsmeyer–Peppas model ($R^2 = 0.793 \pm 0.027$), closely followed by the Higuchi model ($R^2 = 0.773 \pm 0.059$), suggesting that diffusion through the lipid matrix remains the predominant mechanism in the selected formulation.[42]

The diffusional exponent (n) further clarified the transport behavior. Pure curcumin exhibited an n value of 2.092 ± 0.125, indicative of anomalous or non-Fickian transport, likely influenced by its crystalline nature and limited solubility. Meanwhile, CaTS2 showed an n value of 0.301 ± 0.057, consistent with Fickian diffusion, confirming that drug release is primarily governed by concentration-driven diffusion through the reorganized lipid matrix. The higher Higuchi constant observed for CaTS2 ($KH = 1.561 \pm 0.253$) compared with Cur ($KH = 1.083 \pm 0.074$) further supports enhanced diffusion kinetics in the NLC system.[42]

These findings are consistent with the observations reported by Araujo et al, who found that variations in solid-to-liquid lipid ratios and lipid molecular characteristics did not drastically alter the overall release mechanism, which followed predominantly zero-order or Weibull kinetics with Fickian diffusion behavior.[49] In their work, despite differences in NLC composition, the release profiles of curcumin remained similar, highlighting that drug release from NLCs is primarily governed by diffusion through the lipid matrix rather than rapid matrix erosion.

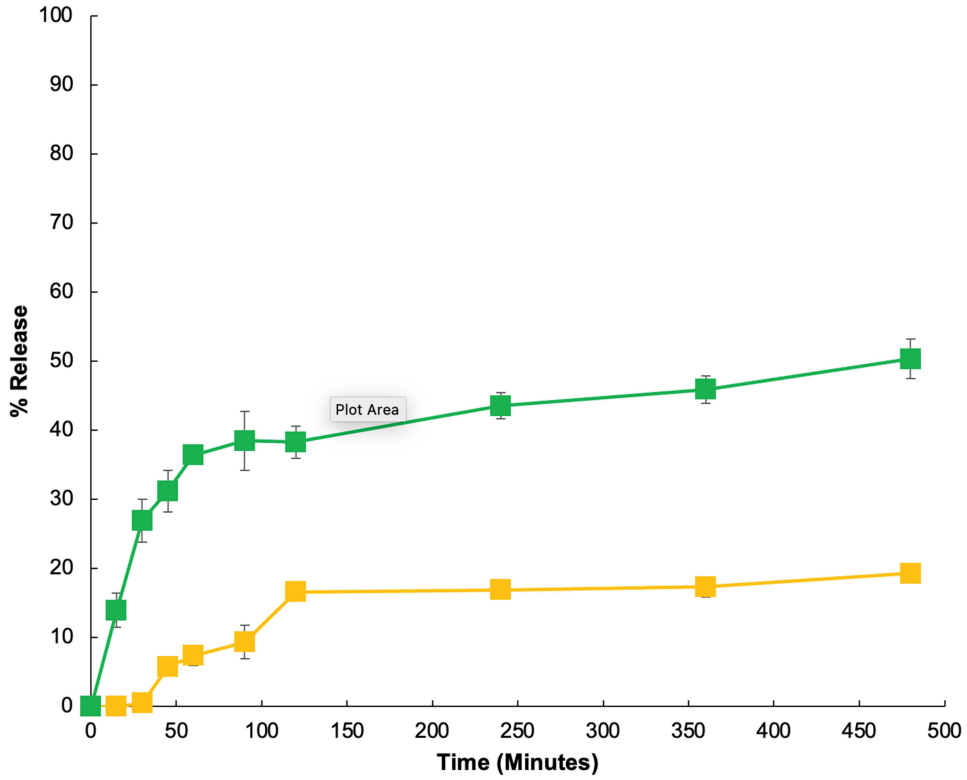

Figure 5 In vitro release profiles of raw curcumin (Orange line) and selected CaTS2 (green line) in phosphate buffer (pH 7.4) at 37 ± 0.5 °C over 480 min. Data are presented as mean ± SD (n = 3). Error bars represent standard deviation.

However, in the present study, the observed differences in release extent suggest that sacha inchi oil may impart a unique modulatory effect on lipid matrix organization. The high degree of unsaturation in sacha inchi oil likely increases lipid fluidity, facilitating faster diffusion of curcumin, while combinations with more crystalline solid lipids may counterbalance this effect, resulting in prolonged drug retention.[63] At the molecular level, the unsaturated fatty acid chains of sacha inchi oil introduce structural discontinuities within the solid lipid framework, thereby enhancing chain mobility and reducing diffusion barriers. This increased lipid dynamics promotes more efficient drug migration from the core to the surrounding medium, explaining the enhanced cumulative release observed.

To quantitatively compare the dissolution profiles, the similarity factor (f_2) was calculated between Cur and CaTS2. The obtained value (f_2 = 29.04) was below the regulatory threshold of 50, indicating that the two release profiles are not similar.[43] This quantitative assessment confirms that incorporation into the NLC system significantly modifies curcumin release behavior, resulting in enhanced and kinetically distinct diffusion characteristics.

Importantly, the developed NLC system was designed to enhance the delivery of curcumin for topical application, particularly for antioxidant and anti-inflammatory purposes. Curcumin is well known for its potent biological activity; however, its poor aqueous solubility and limited skin permeation restrict its therapeutic efficacy. The improved release

Table 3 Release Kinetic Parameters of Curcumin (Cur) and Selected CaTS2 Nanostructured Lipid Carrier Obtained from Zero-Order, First-Order, Higuchi, and Korsmeyer–Peppas Models

Sample	Zero Order		First Order		Higuchi		Korsmeyer-Peppas		
	K_0	R^2	K_1	R^2	K_H	R^2	K_P	n	R^2
Cur	0.038 ± 0.003	0.689 ± 0.067	0.020 ± 0.001	0.731 ± 0.063	1.083 ± 0.074	0.819 ± 0.060	$1.46\times10^{-5} \pm 1.20\times10^{-5}$	2.092 ± 0.125	0.631 ± 0.047
CaTS2	0.054 ± 0.009	0.647 ± 0.062	0.020 ± 0.001	0.675 ± 0.037	1.561 ± 0.253	0.773 ± 0.059	0.178 ± 0.056	0.301 ± 0.057	0.793 ± 0.027

Note: Data are expressed as mean ± SD (n = 3).

profile observed in CaTS2 suggests enhanced drug availability at the application site, which is expected to improve local therapeutic performance. The initial burst release may provide rapid onset of action, while the sustained phase supports prolonged retention in the skin tissue.[64]

The biphasic release pattern observed herein aligns well with the therapeutic rationale of NLC-based delivery systems, where an initial burst may provide a rapid onset of action, followed by sustained release to maintain therapeutic levels.[15] In this context, the NLC system functions as a carrier to overcome solubility limitations and to modulate drug release in a controlled manner, thereby improving curcumin bioavailability in topical formulations.[65] Importantly, the ability to modulate release kinetics through lipid and surfactant selection reinforces the versatility of NLCs as tunable drug delivery platforms. These characteristics are particularly relevant for pharmaceutical applications requiring controlled delivery of poorly soluble bioactives, as well as for cosmetic formulations aimed at sustained antioxidant or anti-inflammatory activity in topical systems. The incorporation of natural, polyunsaturated oils such as sacha inchi oil may therefore offer added functional value by combining structural modulation with intrinsic biological benefits.

Conclusion

Curcumin-loaded nanostructured lipid carriers (NLCs) based on sacha inchi oil were successfully developed using different solid lipids, namely oleum cacao, glyceryl behenate, and glyceryl palmitostearate, in combination with Tween 80, Poloxamer 188, or a Tween 80–Span 80 surfactant system. Physicochemical characterization demonstrated that formulations exhibiting the most favorable characteristics exhibited favorable performance, with particle sizes ranging from 64 to 3110 nm, PDI values below 0.5 indicating relatively homogeneous particle size distribution, and ZP values between −5.2 and −31.63 mV, suggesting varying degrees of colloidal stability under the tested storage conditions. All formulations showed high curcumin entrapment efficiency, approaching 80–90%, confirming the suitability of the NLC system for encapsulating lipophilic compounds. Morphological analysis revealed predominantly spherical particles, while in vitro release studies demonstrated a biphasic release profile characterized by an initial burst release followed by sustained curcumin release, which varied according to lipid and surfactant composition. The inclusion of sacha inchi oil, rich in polyunsaturated fatty acids, may contribute to modulation of lipid matrix organization and diffusion behavior within the NLC system.

From a practical perspective, these findings support the potential application of sacha inchi oil–based NLCs as lipid-based nanocarriers for improving the delivery of poorly soluble bioactive compounds. The developed system shows promise for topical formulations where enhanced solubility, controlled release, and improved local skin availability are required. Overall, these findings demonstrate the feasibility of developing sacha inchi oil–based NLCs represent a promising lipid-based nanocarrier for curcumin delivery and provide a basis for further formulation refinement. However, additional studies incorporating extended stability evaluation, comparative systems, and in vivo investigations are necessary to more comprehensively establish the functional advantages and application potential of this formulation strategy.

Acknowledgments

We would like to extend our gratitude to the Universitas Padjadjaran for funding the APC through the Indonesian Endowment Fund for Education (LPDP) on behalf of the Indonesian Ministry of Higher Education, Science and Technology and managed under the EQUITY Program (Contract No. 4303/B3/DT.03.08/2025 and 3927/UN6.RKT/HK.07.00/2025). In addition, the author(s) used ChatGPT (OpenAI) to assist in proofreading and improving the readability of the initial manuscript draft. After using this tool, the author(s) carefully reviewed and edited the content as needed and take full responsibility for the content of the published article.

Funding

This work was supported by the Industrial and/or Government Institution Collaboration Grant (RKIIP), Universitas Padjadjaran, Fiscal Year 2025, under the Implementation Agreement for Research Activities Number 4217/UN6.3.1/PT.00/2025.

Disclosure

The authors report no conflicts of interest in this work.

References

1. Iweala EJ, Uche ME, Dike ED, et al. Curcuma longa (Turmeric): ethnomedicinal uses, phytochemistry, pharmacological activities and toxicity profiles—A review. *Pharmacol Res-Mod Chin Med*. 2023;6:100222. doi:10.1016/j.prmcm.2023.100222
2. Vollmannová A, Bojňanská T, Musilová J, Lidiková J, Cifrová M. Quercetin as one of the most abundant represented biological valuable plant components with remarkable chemoprotective effects-A review. *Heliyon*. 2024;10(12):e33342. doi:10.1016/j.heliyon.2024.e33342
3. El-Saadony MT, Yang T, Korma SA, et al. Impacts of turmeric and its principal bioactive curcumin on human health: pharmaceutical, medicinal, and food applications: a comprehensive review. *Front Nutr*. 2023;9:1040259. doi:10.3389/fnut.2022.1040259
4. Koop BL, da Silva MN, da Silva FD, et al. Flavonoids, anthocyanins, betalains, curcumin, and carotenoids: sources, classification and enhanced stabilization by encapsulation and adsorption. *Food Res Int*. 2022;153:110929. doi:10.1016/j.foodres.2021.110929
5. Urošević M, Nikolić L, Gajić I, Nikolić V, Dinić A, Miljković V. Curcumin: biological activities and modern pharmaceutical forms. *Antibiotics*. 2022;11(2):135. doi:10.3390/antibiotics11020135
6. Sohn SI, Priya A, Balasubramaniam B, et al. Biomedical applications and bioavailability of curcumin—An updated overview. *Pharmaceutics*. 2021;13(12):2102. doi:10.3390/pharmaceutics13122102
7. Islam S, Ahmed MMS, Islam MA, Hossain N, Chowdhury MA. Advances in nanoparticles in targeted drug delivery-A review. *Results Surf Interf*. 2025;19:100529.
8. Jafar G, Salsabilla S, Santoso R. Original article development and characterization of compritol ato ® base in nanostructured lipid carriers formulation with the probe sonication method. *Int J Appl Pharm*. 2022;14(4):64–66.
9. Yeo S, Kim MJ, Shim YK, Yoon I, Lee WK. Solid lipid nanoparticles of curcumin designed for enhanced bioavailability and anticancer efficiency. *ACS Omega*. 2022;7(40):35875–35884. doi:10.1021/acsomega.2c04407
10. Jafar G, Fira PA, Muhsinin S, Kencana B. Formulation and characterization of tretinoin nanostructured lipid carriers using apifil and cremophore. *Indonesian J Pharm*. 2025;5(3):477–484.
11. Thuy VN, Van TV, Dao AH, Lee BJ, Lee B-J. Nanostructured lipid carriers and their potential applications for versatile drug delivery via oral administration. *OpenNano*. 2022;8:100064. doi:10.1016/j.onano.2022.100064
12. Mall J, Naseem N, Haider MF, Rahman MA, Khan S, Siddiqui SN. Nanostructured lipid carriers as a drug delivery system: a comprehensive review with therapeutic applications. *Intelligent Pharm*. 2024.
13. Syed Azhar SNA, Ashari SE, Zainuddin N, Hassan M. Nanostructured lipid carriers-hydrogels system for drug delivery: nanohybrid technology perspective. *Molecules*. 2022;27(1):289. doi:10.3390/molecules27010289
14. Viegas C, Patrício AB, Prata JM, Nadhman A, Chintamaneni PK, Fonte P. Solid lipid nanoparticles vs. nanostructured lipid carriers: a comparative review. *Pharmaceutics*. 2023;15(6):1593. doi:10.3390/pharmaceutics15061593
15. Khan S, Sharma A, Jain V. An overview of nanostructured lipid carriers and its application in drug delivery through different routes. *Adv Pharm Bull*. 2023;13(3):446–460. doi:10.34172/apb.2023.056
16. Espinosa-Olivares MA, Delgado-Buenrostro NL, Chirino YI, Trejo-Márquez MA, Pascual-Bustamante S, Ganem-Rondero A. Nanostructured lipid carriers loaded with curcuminoids: physicochemical characterization, in vitro release, ex vivo skin penetration, stability and antioxidant activity. *Eur J Pharm Sci*. 2020;155:105533. doi:10.1016/j.ejps.2020.105533
17. Elmowafy M, Al-Sanea MM. Nanostructured lipid carriers (NLCs) as drug delivery platform: advances in formulation and delivery strategies. *Saudi Pharm J*. 2021;29(9):999–1012. doi:10.1016/j.jsps.2021.07.015
18. Redjeki SG, Hulwana AF, Aulia RN, Maya I, Chaerunisaa AY, Sriwidodo S. Sacha Inchi (Plukenetia volubilis): potential bioactivity, extraction methods, and microencapsulation techniques. *Molecules*. 2025;30(1):160. doi:10.3390/molecules30010160
19. Cárdenas DM, Gómez Rave LJ, Soto JA. Biological activity of sacha inchi (Plukenetia volubilis Linneo) and potential uses in human health: a review. *Food Technol Biotechnol*. 2021;59(3):253–266. doi:10.17113/ftb.59.03.21.6683
20. Jamaludin J. The Sacha Inchi (Plukenetia volubilis) research trends for health. *Jurnal EduHealth*. 2025;16(01):344–351.
21. Henao-Ardila A, Quintanilla-Carvajal MX, Moreno FL. Emulsification and stabilisation technologies used for the inclusion of lipophilic functional ingredients in food systems. *Heliyon*. 2024;10(11):e32150. doi:10.1016/j.heliyon.2024.e32150
22. Murasiewicz H, Illienko K. Liquid-liquid two phase-system stabilized by tween 40 and 80 surfactants: multiparametric study. *Pol J Chem Technol*. 2024;26(1):51–63. doi:10.2478/pjct-2024-0006
23. Chen W, Stolz S, Wegbecher V, et al. The degradation of poloxamer 188 in buffered formulation conditions. *AAPS Open*. 2022;8(1):5. doi:10.1186/s41120-022-00055-4
24. Putri AIE, Ariyanto HD. Effect of hydrophilic-lipophilic balance (HLB) value on the stability of cosmetic lotion based on walnut oil (Canarium Indicium L.) oil-in-water emulsion. *J Vocational Stud Appl Res*. 2022;4(2):53–60. doi:10.14710/jvsar.v4i2.15376
25. Madania MN, Ningsih Z, Devi AF, Mardiana D, Andayani U. The effect of surfactant on the characteristics of curcumin-loaded nanostructured lipid carriers: fluorescence and stability study. *J Pure Appl Chemistry Res*. 2025;14(1):1–12. doi:10.21776/ub.jpacr.2025.014.01.7933
26. Jafar G, Sucipto YK, Supriadi D. Development of the formula and characterization of tretinoin nanostructured lipid carriers (NLC) with precirol ® ato5 using the sonicator probe method. *Indones J Pharm Sci Technol*. 2024;10(6):62–67.
27. Akbari J, Saeedi M, Ahmadi F, et al. Solid lipid nanoparticles and nanostructured lipid carriers: a review of the methods of manufacture and routes of administration. *Pharm Dev Technol*. 2022;27(5):525–544. doi:10.1080/10837450.2022.2084554
28. Almaamari JNS. Pharmacological effects and pharmaceutical dosage forms development of aloe vera. *Jurnal Farmasi Sains dan Terapan*. 2021;8(2):85–90.
29. Rao H, Rao I, Ahmad S, Madni A, Ahmad I. Compritol®-based solid lipid nanoparticles of desvenlafaxine prepared by ultrasonication-assisted hot-melt encapsulation to modify its release. *Nanomedicine*. 2024;19(11):965–978. doi:10.2217/nnm-2023-0229

30. Wu KW, Sweeney C, Dudhipala N, et al. Primaquine loaded solid lipid nanoparticles (SLN), nanostructured lipid carriers (NLC), and nanoemulsion (NE): effect of lipid matrix and surfactant on drug entrapment, in vitro release, and ex vivo hemolysis. *AAPS Pharm Sci Tech*. 2021;22(7):240. doi:10.1208/s12249-021-02108-5
31. da Silva MG, de Godoi KRR, Gigante ML, Cardoso LP, Ribeiro APB. Developed and characterization of nanostructured lipid carriers containing food-grade interesterified lipid phase for food application. *Food Res Int*. 2022;155:111119. doi:10.1016/j.foodres.2022.111119
32. Brusač E, Jeličić ML, Cvetnić M, Amidžić Klarić D, Nigović B, Mornar A. A comprehensive approach to compatibility testing using chromatographic, thermal and spectroscopic techniques: evaluation of potential for a monolayer fixed-dose combination of 6-mercaptopurine and folic acid. *Pharmaceuticals*. 2021;14(3):274. doi:10.3390/ph14030274
33. Beloqui A, Memvanga PB, Coco R, et al. A comparative study of curcumin-loaded lipid-based nanocarriers in the treatment of inflammatory bowel disease. *Colloids Surf B Biointerf*. 2016;143:327–335. doi:10.1016/j.colsurfb.2016.03.038
34. Khosa A, Reddi S, Saha RN. Nanostructured lipid carriers for site-specific drug delivery. *Biomed Pharmacother*. 2018;103:598–613. doi:10.1016/j.biopha.2018.04.055
35. Suyuti A, Hendradi E, Purwanti T. Physicochemical characteristics, entrapment efficiency, and stability of nanostructured lipid carriers loaded coenzyme Q10 with different lipid ratios. *J Res Pharm*. 2023;27(3):1134–1142. doi:10.29228/jrp.404
36. Bolívar-Jacobo NA, Reyes-Villagrana RA, Espino-Solís GP, et al. The effects of a high-intensity ultrasound on the fermentative activity and kinetic growth of Lactobacillus acidophilus and Lactobacillus helveticus. *Fermentation*. 2023;9(4):356. doi:10.3390/fermentation9040356
37. Elkhateeb O, Badawy MEI, Tohamy HG, Abou-Ahmed H, El-Kammar M, Elkhenany H. Curcumin-infused nanostructured lipid carriers: a promising strategy for enhancing skin regeneration and combating microbial infection. *BMC Vet Res*. 2023;19(1). doi:10.1186/s12917-023-03774-2
38. Schmidt M, Hopfhauer S, Schwarzenbolz U, Böhm V. High-pressure processing of kale: effects on the extractability, in vitro bioaccessibility of carotenoids & vitamin E and the lipophilic antioxidant capacity. *Antioxidants*. 2021;10(11):1688. doi:10.3390/antiox10111688
39. Chen J, Li S, Zheng Q, et al. Preparation of solid lipid nanoparticles of cinnamaldehyde and determination of sustained release capacity. *Nanomaterials*. 2022;12(24):4460. doi:10.3390/nano12244460
40. Dudhipala N, Ettireddy S, Youssef AAA, Puchchakayala G. Cyclodextrin complexed lipid nanoparticles of irbesartan for oral applications: design, development, and in vitro characterization. *Molecules*. 2021;26(24):7538. doi:10.3390/molecules26247538
41. Sebe I, Zsidai L, Zelkó R. Novel modified vertical diffusion cell for testing of in vitro drug release (IVRT) of topical patches. *HardwareX*. 2022;11:e00293. doi:10.1016/j.ohx.2022.e00293
42. Adepu S, Ramakrishna S. Controlled drug delivery systems: current status and future directions. *Molecules*. 2021;26(19):5905. doi:10.3390/molecules26195905
43. Shiek abdul kadhar Mohamed Ebrahim HR, Chungath TT, Sridhar K, et al. Development and validation of a discriminative dissolution medium for a poorly soluble nutraceutical tetrahydrocurcumin. *Turk J Pharm Sci*. 2021;18(5):565–573. doi:10.4274/tjps.galenos.2021.91145
44. Mendoza-Almeida T, Ramírez-Roca EG, Suárez-Cunza S. Fatty acid profile and effect of Plukenetia volubilis L. (sacha inchi) oil on lipid metabolism in rats fed a high-fat diet. *Braz J Med Biol Res*. 2025;58. doi:10.1590/1414-431X2025e14684
45. Krambeck K, Silva V, Silva R, et al. Design and characterization of Nanostructured lipid carriers (NLC) and Nanostructured lipid carrier-based hydrogels containing Passiflora edulis seeds oil. *Int J Pharm*. 2021;600:120444. doi:10.1016/j.ijpharm.2021.120444
46. Shah RM, Jadhav SR, Bryant G, Kaur IP, Harding IH. On the formation and stability mechanisms of diverse lipid-based nanostructures for drug delivery. *Adv Colloid Interface Sci*. 2025;338:103402. doi:10.1016/j.cis.2025.103402
47. Luu NA, To TT, Tran NH, et al. Optimization of plant oil-based nanoemulsions prepared via phase inversion temperature and evaluation of their antioxidant capacity. *Oil Crop Sci*. 2025;10(3):194–204. doi:10.1016/j.ocsci.2025.02.004
48. Koroleva M, Portnaya I, Mischenko E, Abutbul-Ionita I, Kolik-Shmuel L, Danino D. Solid lipid nanoparticles and nanoemulsions with solid shell: physical and thermal stability. *J Colloid Interface Sci*. 2022;610:61–69. doi:10.1016/j.jcis.2021.12.010
49. Araujo VHS, da Silva PB, Szlachetka IO, et al. The influence of NLC composition on curcumin loading under a physicochemical perspective and in vitro evaluation. *Colloids Surf a Physicochem Eng Asp*. 2020;602:125070. doi:10.1016/j.colsurfa.2020.125070
50. Lakhani P, Patil A, Taskar P, Ashour E, Majumdar S. Curcumin-loaded nanostructured lipid carriers for ocular drug delivery: design optimization and characterization. *J Drug Deliv Sci Technol*. 2018;47:159–166. doi:10.1016/j.jddst.2018.07.010
51. Madane RG, Mahajan HS. Curcumin-loaded nanostructured lipid carriers (NLCs) for nasal administration: design, characterization, and in vivo study. *Drug Deliv*. 2016;23(4):1326–1334. doi:10.3109/10717544.2014.975382
52. Bao Y, Pignitter M. Mechanisms of lipid oxidation in water-in-oil emulsions and oxidomics-guided discovery of targeted protective approaches. *Compr Rev Food Sci Food Saf*. 2023;22(4):2678–2705. doi:10.1111/1541-4337.13158
53. Kamaly N, Yameen B, Wu J, Farokhzad OC. Degradable controlled-release polymers and polymeric nanoparticles: mechanisms of controlling drug release. *Chem Rev*. 2016;116(4):2602–2663. doi:10.1021/acs.chemrev.5b00346
54. Duan Y, Dhar A, Patel C, et al. A brief review on solid lipid nanoparticles: part and parcel of contemporary drug delivery systems. *RSC Adv*. 2020;10(45):26777–26791. doi:10.1039/D0RA03491F
55. Varga N, Herczeg Z, Kókai KP, Juhász Á, Csapó E. Effect of flow conditions for the reproducible construction of colloidal drug carriers based on polycaprolactone. *Colloids Surf a Physicochem Eng Asp*. 2025;720:137146. doi:10.1016/j.colsurfa.2025.137146
56. Correia EL, Thakur S, Ervin A, Shields E, Razavi S. Adsorption of surfactant molecules onto the surface of colloidal particles: case of like-charged species. *Colloids Surf a Physicochem Eng Asp*. 2023;676:132142. doi:10.1016/j.colsurfa.2023.132142
57. Zhang Z, Marie Woys A, Hong K, et al. Adsorption of non-ionic surfactant and monoclonal antibody on siliconized surface studied by neutron reflectometry. *J Colloid Interface Sci*. 2021;584:429–438. doi:10.1016/j.jcis.2020.09.110
58. Sinsuebpol C, Changsan N. Effects of ultrasonic operating parameters and emulsifier system on sacha inchi oil nanoemulsion characteristics. *J Oleo Sci*. 2020;69(5):437–448. doi:10.5650/jos.ess19193
59. Sakellari GI, Zafeiri I, Batchelor H, Spyropoulos F. Formulation design, production and characterisation of solid lipid nanoparticles (SLN) and nanostructured lipid carriers (NLC) for the encapsulation of a model hydrophobic active. *Food Hydrocoll Health*. 2021;1:100024. doi:10.1016/j.fhfh.2021.100024
60. Darley E, Singh JKD, Surace NA, Wickham SFJ, Baker MAB. The fusion of lipid and DNA nanotechnology. *Genes*. 2019;10(12):1001. doi:10.3390/genes10121001

61. Suhandi C, Wilar G, Lesmana R, et al. Propolis-based nanostructured lipid carriers for α-mangostin delivery: formulation, characterization, and in vitro antioxidant activity evaluation. *Molecules*. 2023;28(16):6057. doi:10.3390/molecules28166057
62. Haider M, Abdin SM, Kamal L, Orive G. Nanostructured lipid carriers for delivery of chemotherapeutics: a review. *Pharmaceutics*. 2020;12 (3):288. doi:10.3390/pharmaceutics12030288
63. Harayama T, Antonny B. Beyond fluidity: the role of lipid unsaturation in membrane function. *Cold Spring Harb Perspect Biol*. 2023;15(7): a041409. doi:10.1101/cshperspect.a041409
64. Suhandi C, Wilar G, Mohammed AFA, et al. Propolis-based nanostructured lipid carrier of α-mangostin for promoting diabetic wound healing in alloxan-induced mice. *J Inflamm Res*. 2025;18:7443–7457. doi:10.2147/JIR.S525243
65. Wathoni N, Suhandi C, Elamin KM, et al. Advancements and challenges of nanostructured lipid carriers for wound healing applications. *Int J Nanomed*. 2024;19:8091–8113. doi:10.2147/IJN.S478964